

Effect of fluctuations on the Geodesic rule for topological defect formation

Sanatan Digal^{1,2,*} and Vinod Mamale^{1,2,†}

¹*The Institute of Mathematical Sciences, Chennai 600113, India*

²*Homi Bhabha National Institute, Training School Complex,
Anushakti Nagar, Mumbai 400085, India*

Abstract

At finite temperature, the field along a linear stretch of correlation length size is supposed to trace shortest path in the field space given the two end points, known as the Geodesic rule. In this study we compute the probability that the field variations over distances of correlation length follow the Geodesic rule in theories with $O(2)$ global symmetry. We consider a model of ferromagnetic $O(2)$ spins and a complex ϕ^4 theory. The computations are carried out on an ensemble of equilibrium configurations at finite temperatures generated using Monte Carlo simulations. The numerical results suggest that, for temperatures relevant for the studies of topological defect formation during 2nd order phase transition, there is a significant deviation from the Geodesic rule. We also study the equilibrium density and distribution of vortices in $O(2)$ spins in two dimensions and compare with the Kibble-Zurek Mechanism of defect formation.

* digal@imsc.res.in

† mvinod@imsc.res.in

I. INTRODUCTION

Topological defects arise in a wide variety of systems ranging from table-top experiments in condensed matter systems[1–7] to theories of the early Universe, extremely dense stars etc.[8–10]. Topological defects mostly form during phase transitions accompanied by spontaneous breaking (SSB) of discrete or continuous symmetries. These defects can also be excited in the SSB phase by external stimulations [11]. The type of topological defects that are possible depends on the corresponding homotopy group and the spatial dimensions, irrespective of the energetics involved [12–14]. The processes of formation and evolution of these defects have been extensively studied in the literature. There are many theoretical as well as experimental studies available on the formation of topological defects in condensed matter systems [15, 16]. In the case of high energy physic systems the studies are mostly theoretical. However since topological considerations play a dominant role in their formation and evolution, ideas proposed for high energy physics systems have been tested in condensed matter systems.

The theory of formation of topological defects was first proposed in the context of the early Universe by T. W. B. Kibble, known as the Kibble-Mechanism(KM) [17]. The Kibble-Mechanism is based on two postulates. In the immediate aftermath of a phase transition the order parameter (OP) in physical space takes values from the order parameter space (OPS). According to the first postulate of KM, immediately after a SSB phase transition the physical space splits into domains, inside of which the OP is roughly uniform. The second postulate, which is also known as the “Geodesic Rule”, states that in between adjacent domains OP field interpolates along the shortest path in the OPS [18]. Given an OPS these two postulates can be applied to make definite predictions such as the minimum number of domains required to form a defect, defect densities and defect correlations etc. [19, 20]. For example, in two dimensions a minimum of three domains are required to form a vortex or anti-vortex, which is usually located near the junction of these. The probability of formation is estimated to be 0.25. According to the Kibble Mechanism the formation of defects for a given OPS, spatial dimensions, and the nature of phase transition, does not depend on the energy scales involved, i.e whether in a condensed matter system, in high energy systems or in the early Universe.

The Kibble mechanism has been very successful in describing the formation of topological

defects during a first order transition. In a first order phase transition, bubbles of SSB phase nucleate in the background of symmetric phase [21]. The bubbles with uniform OP always dominate during the nucleation as these correspond to least action. These bubbles can be identified with the domains proposed in the Kibble Mechanism. These bubbles grow, collide/coalesce with one another converting the symmetric phase into the SSB phase. It has been observed in numerical experiments that when two bubbles collide, the OP variation from one bubble to the other interpolates along the shortest path in the OPS validating the geodesic rule of the Kibble mechanism [21, 22]. Though there can be exceptions to this when kinematics allow energetic bubble collisions or there is a small explicit symmetry breaking present apart from the SSB [23–25].

In a second order phase transition formation of topological defects is described by the Kibble-Zurek mechanism [12]. In this case it becomes necessary to incorporate the phenomenon of critical slowing down in the Kibble Mechanism which was first pointed out by Zurek. Zurek argued that in a second order phase transition as the system temperature approaches the critical temperature (T_c) from above, the dynamics of the field almost freezes as soon as it enters the regime of critical slowing down [$T_c + \epsilon_1, T_c - \epsilon_2$]. When the system exits this regime, the field configuration still corresponds to temperature $T_c + \epsilon_1$, even though the temperature is equal to or below $T_c - \epsilon_2$. The field configuration at $T = T_c + \epsilon_1$ is laid out using the two postulates of Kibble mechanism. If the temperature of the system were to remain fixed at $T_c + \epsilon_1$ the domains will keep fluctuating and there will be continuous creation and annihilation of unstable topological defects. Since the system temperature $T \leq T_c - \epsilon_2$, i.e the effective potential now has a non trivial OPS, the field inside the domains will roll down to the corresponding nearest point on the OPS. In this process the topological defects will become stable.

Though the two postulates of the Kibble Mechanism and the Kibble-Zurek Mechanism, have been very successful in describing the formation and dynamics of topological defects their validity, in particular that of the Geodesic rule has never been tested in the case of *2nd* order phase transition. It is argued that the Geodesic rule follows from free energy considerations, i.e when the field variation over the distances traces shortest path on the OPS the energy and free energy are minimised. However, the same can be achieved by maximising the entropy. A definitive answer to whether there are deviations to Geodesic rule can come only from the simulations of the partition function. In this work we compute the deviations

from the Geodesic rule in the $O(2)$ -spin model in two and three spatial dimensions. In this model the spins take values from an unit circle. We also consider ϕ^4 theory with $U(1) \equiv O(2)$ symmetry in three spatial dimensions to see the effect of radial/magnitude fluctuations on the Geodesic rule. In the relevant temperature range of interest the ϕ field takes values from a circular band in the complex ϕ -plane.

The computations involve Monte Carlo simulation of the lattice partition function of both the models. At a given temperature the correlation length ξ is computed. The conventional definition of ξ is not suitable for the Kibble Mechanism as the correlation of the field at ξ separations does not vanish. Therefore we define ξ_{KM} such that field correlation approximately vanishes over ξ_{KM} separations. It is found that ξ_{KM} is significantly larger than ξ . Once ξ and ξ_{KM} are computed the field configuration over a stretch of ξ_{KM} is mapped onto the field space. Finding length of the image trajectory in the field space requires assumption of the Geodesic rule for variations of the field between nearest neighbour (NN) on the lattice. The simulations results for both the models show significant deviations from the Geodesic rule. The deviation over ξ distances is found to be above 20%. Over ξ_{KM} the trajectories no longer prefer the Geodesic path in the field space. Even the maximal violation of the Geodesic rule largely underestimates the defect densities. This is possibly due to dominance of defects arising from thermal fluctuations. These results suggest that even over ξ_{KM} fluctuations dominate the field dynamics.

The paper is organised as follows. In section-II and section-III, numerical calculations to determine the validity of geodesic rule are presented for the $O(2)$ -spin model and ϕ^4 theory respectively. The conclusions are presented in section-IV.

II. GEODESIC RULE IN $O(2)$ -SPIN MODEL

The $O(2)$ -spin model, also known as the XY -model, is a toy spin model on the lattice [26]. Each of the spins, \vec{s}_i at the site i , is a two component unit vector. The spin \vec{s}_i can also be represented by an angle θ_i such that $\vec{s}_i = (\cos\theta_i, \sin\theta_i)$. The Hamiltonian,

$$H = -J \sum_{\langle ij \rangle} \vec{s}_i \cdot \vec{s}_j, \quad (1)$$

includes ferromagnetic coupling ($J > 0$) between the i -th and j -th spins which are NN's. The $O(2)$ -symmetry corresponds to global rotations of the spins which preserve the Hamiltonian. For simplicity, external field breaking the $O(2)$ symmetry explicitly is not considered in the present study. The expression for the partition function is given by,

$$\mathcal{Z} = \int \prod_i^N d\vec{s}_i \text{Exp}[\beta \sum_{\langle ij \rangle} \vec{s}_i \cdot \vec{s}_j]. \quad (2)$$

$\beta = J/\kappa T$, where κ and T are the Boltzmann constant and temperature respectively. For convenience T is considered in units of J/κ . It is well known that in three or higher dimensions the system of lattice spins undergoes a 2nd order ferromagnetic-paramagnetic transition at critical temperature T_c . The order parameter for this transition is given by,

$$\vec{M} = \left\langle \frac{1}{N} \sum_i \vec{s}_i \right\rangle. \quad (3)$$

The magnitude of \vec{M} acquires non-zero value for temperatures, $T \leq T_c$, which leads to SSB of $O(2)$ symmetry. The symmetry broken phase allows for existence of stable topological defects corresponding to the first homotopy group $\pi_1(S^1) \equiv Z$. These defects can exist even above T_c but are unstable. In the case of two physical dimensions there is no magnetisation transition due to dominance of the Goldstone modes. Interestingly the system undergoes the well known Kosterlitz-Thouless(KT) transition[26]. The spin system consists of a network of vortices at all temperatures. The two phases are characterised by how the vortices interact. The high temperature phase is described by a screened Coulomb gas and a strongly interacting system below the KT transition. Though the two dimensional system is not directly relevant for the formation of topological defects via the Kibble-Zurek mechanism, the distribution of vortices at high temperature serves as an instructive example. The results of the deviation from the Geodesic rule in two and three dimensions are very similar. Also there is no reason to expect that the Geodesic rule will not hold in the case of two spatial dimensions.

Simulation of the partition function, Eq.2, involves mainly generating statistically significant spin configurations using Monte Carlo methods at various temperatures above $T > T_c$. To generate the configurations the standard metropolis algorithm[27] is used. In this al-

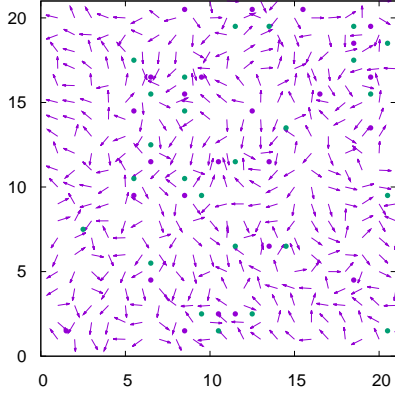


FIG. 1. A sampled spin configuration at $T = 1.6T_c$.

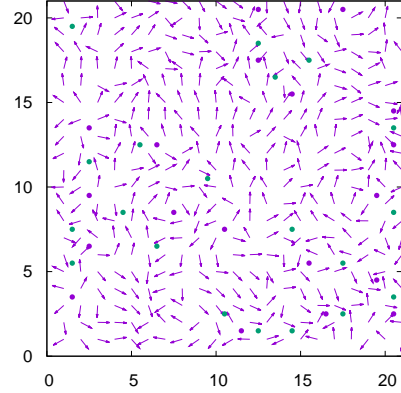


FIG. 2. A sampled spin configuration at $T = 1.4T_c$.

gorithm the spin \vec{s}_i at site i is rotated by an angle θ randomly chosen between $0 - 2\pi$ to obtain \vec{s}'_i . The move, $\vec{s}_i \rightarrow \vec{s}'_i$ is accepted if the change in the energy $\Delta E = E' - E < 0$. If $\Delta E > 0$ then the move is accepted with probability $Exp(-\beta\Delta E)$. While the spin \vec{s}_i is being updated, the rest of the spins are held fixed. A sweep constitutes the sequential updating of all the spins. Since a new spin configurations is obtained from an old one, there is non-zero autocorrelation between them. To reduce this auto-correlation to a reasonable level a configuration is accepted for computations after about 10 sweeps. For simplicity, a square lattices ($N = N_s \times N_s$) and a cubic lattice ($N = N_s \times N_s \times N_s$) are considered in 2 and 3- dimensions respectively. In Fig.1 and Fig.2 show a small part of typical 2-dimensional spin configuration generated at temperature $T = 1.43$ and $T = 1.25$ respectively. In these figures the purple dots represent vortices and green dots represent anti-vortices. The spin configuration shown in Fig.1 has more fluctuations compared to configuration in Fig.2 as the temperature is higher for the former. The larger fluctuations lead to higher defect density, so it grows with temperature.

A. Calculation of ξ and ξ_{KM}

Conventionally the correlation length ξ is obtained from the correlation function,

$$c(r) = \langle \vec{s}_i \cdot \vec{s}_j \rangle - \langle \vec{s}_i \rangle \cdot \langle \vec{s}_j \rangle, \quad r = |\mathbf{r}_i - \mathbf{r}_j|, \quad (4)$$

of spins \vec{s}_i and \vec{s}_j located at \mathbf{r}_i and \mathbf{r}_j respectively. For large r , $c(r)$ is expected to decay as $\sim \text{Exp}[-r/\xi(T)]$. Clearly at $r = \xi$, $c(r) \sim 1/e$, consequently \vec{s}_i can not take values independent of \vec{s}_j and vice-versa. For $T = 1.18$, $\xi \simeq 4.4$ in lattice units. At ξ separations, the probability that the relative angle $\Delta\theta = \min[|\theta_i - \theta_j|, 2\pi - |\theta_i - \theta_j|]$ between \vec{s}_i and \vec{s}_j is below $\pi/2$ is $\sim 65\%$, i.e $\langle \Delta\theta \rangle \neq \pi/2$ and $\langle \theta_i \theta_j \rangle \neq \pi^2$. According to the Kibble Mechanism $\Delta\theta$, between two adjacent domains, can take any value between $0 - \pi$ with uniform probability. Consequently, $\langle \Delta\theta \rangle = \pi/2$ or $\langle \theta_i \theta_j \rangle = \pi^2$. Therefore ξ does not accurately describe the size of the domains prescribed in the Kibble Mechanism. We define ξ_{KM} as the least physical separation at which the two spins \vec{s}_i and \vec{s}_j are not correlated, i.e $c(\xi_{KM}) \simeq 0$. At $T = 1.18$, it so happens that ξ_{KM} is larger than ξ by a factor of ~ 5 .

B. The Geodesic rule over ξ and ξ_{KM} separations

The calculations to check the validity or the deviations of the Geodesic rule necessitates that given a configuration of the field along a linear stretch in physical space is mapped to a trajectory in the field space. Since the field is defined only on the lattice grid, the image in the field space in the present context will just be a set of points in the field space. A continuous path needs to be drawn in the field space such that the points corresponding to spins at NN points in physical space are joined by a continuous line. We assume that the field variation between NN points follows the Geodesic rule and accordingly draw segments of the trajectory in the field space. We expect this assumption to be valid for the temperatures we consider as there is always non-zero correlation between NN points. We mention here that the Geodesic rule is taken into account while discretising a continuum theory on the lattice. In numerical simulations of topological defects this rule is used locate as well as compute the windings of the defects.

In the present case the field space or the OPS is a circle. Note that this circle can be characterised by an angular variable θ which can take any value in $[0 - 2\pi]$ with the identification of $\theta = 0$ and $\theta = 2\pi$. The field configuration along a straight line from \mathbf{r}_i to \mathbf{r}_j is mapped to a trajectory on the circle. The spins \vec{s}_i and \vec{s}_j are mapped to the two end points, θ_i and θ_j respectively on the OPS. If the Geodesic rule were valid then the length, $\Delta\theta_{ij}$, of this trajectory will be minimum of $|\theta_i - \theta_j|$ and $2\pi - |\theta_i - \theta_j|$, i.e $\Delta\theta_{ij} = \min[|\theta_i - \theta_j|, 2\pi - |\theta_i - \theta_j|]$.

The length of the trajectory corresponding to the field configuration from \mathbf{r}_i to \mathbf{r}_j is given by the absolute value of,

$$\eta_{ij}(r) = \sum_{k=i}^{j-1} \alpha_k \Delta\theta_{k+1,k}, \quad \Delta\theta_{k+1,k} = \min [|\theta_{k+1} - \theta_k|, 2\pi - |\theta_{k+1} - \theta_k|]. \quad (5)$$

$\alpha_k = +1(-1)$, if following the Geodesic rule the trajectory traces a path clockwise(anti-clockwise) in the field space as one goes from the lattice site \mathbf{r}_k to \mathbf{r}_{k+1} . Note that $\eta_{ij}(r)$ corresponds to net variation of angle θ of the spins over r separation. In case $\Delta\theta_{ij} \neq \eta_{ij}$, it is counted as the deviation from the geodesic rule. This computation is repeated for different values of $r = 2, 3, \dots, \xi_{KM}$ resulting in the function $d(r)$ which gives the deviation from the Geodesic rule at separation r .

In figure 3 we show an example of the field configurations along a linear stretch of ξ_{KM} for $T = 1.43$. $\xi_{KM} = 12$ for this T . The corresponding image in the OPS is shown in figure 4. The two end points correspond to $\theta_1 \simeq 0.325\pi$ and $\theta_{13} \simeq 0.292\pi$, with $\Delta\theta_{1,13} = 0.033\pi$. $\eta_{1,13}$ in this case turns out to be $2\pi - \Delta\theta_{1,13} = 1.967\pi$; which does not correspond to the shortest path. This configuration is an example where the Geodesic rule is violated. In figures 5 another configuration is shown for the same T . The corresponding image map is shown in 6. The endpoints for this configuration are; $\theta_1 \simeq 1.76\pi$ and $\theta_{13} \simeq 0.05\pi$. In this case $\Delta\theta_{1,13} = .29\pi$ but $\eta_{1,13}$ is found to be 2.29π . This trajectory not only violates the Geodesic rule but also winds the field space, i.e OPS, once. This implies that for given two end points in the field space there are many ways in which geodesic rule can be violated but there is only one way it is followed.

The Fig.7 and Fig.8 show the probability of deviation from the geodesic rule vs r at various temperatures in two and three dimensional systems respectively. For simplicity this calculation was carried out along the x and y directions only. The results were found to be independent of directions. The results show that the probability of deviation increases with separation r and temperature. The upper points on the curves for different temperatures correspond to the deviation at $r = \xi_{KM}$. Note that the deviation at $r = \xi_{KM}$ increases as we approach T_c from above. This is because ξ_{KM} diverges at T_c . The larger the ξ_{KM} , there are more possibilities to trace different paths between two end points. It is observed that paths with multiple windings around the OPS are possible. For comparison the deviation at the separations $r = \xi$ is also shown in these figures, indicated by blue dots on the different

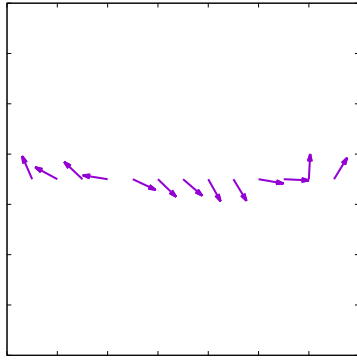


FIG. 3. A configuration spins over length ξ in physical space.

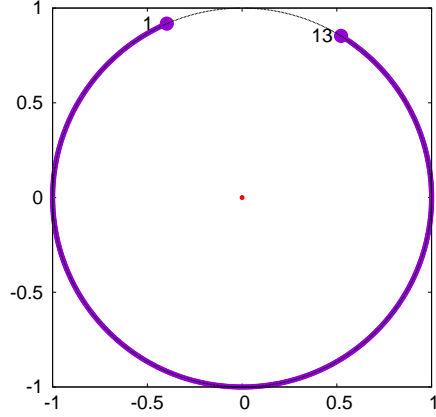


FIG. 4. The corresponding trajectory $\eta_{1,13}$ defined in Eq.(5) on the OPS.

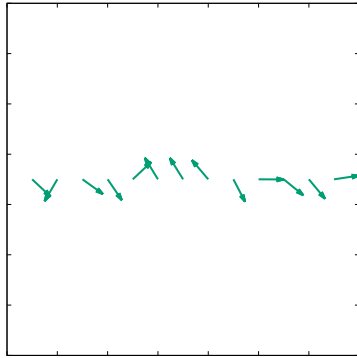


FIG. 5. A configuration spins over length ξ in physical space.

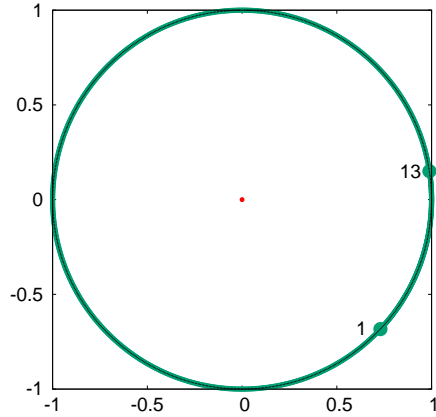


FIG. 6. The corresponding trajectory $\eta_{1,13}$ defined in Eq.(5) on the OPS.

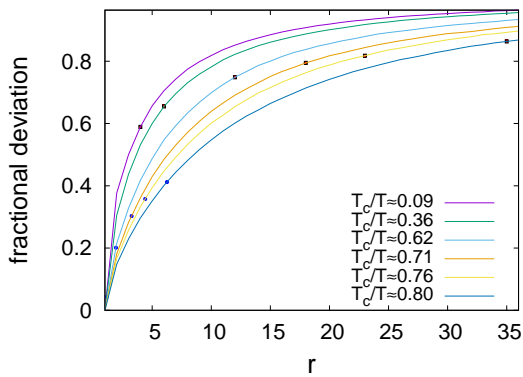


FIG. 7. Geodesic rule deviation in $2D-XY$ model with lattice distance.

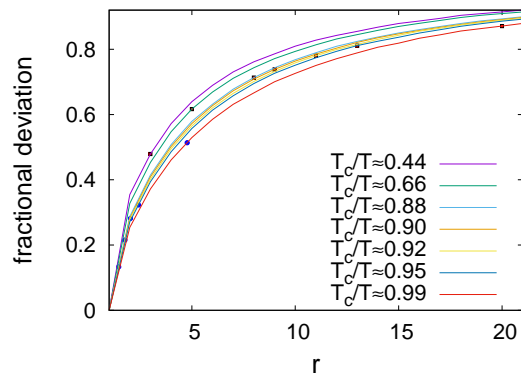


FIG. 8. Geodesic rule deviation in $3D-XY$ model with lattice distance.

curves. Though, this deviation is smaller than that at $r = \xi_{KM}$ but is still significant.

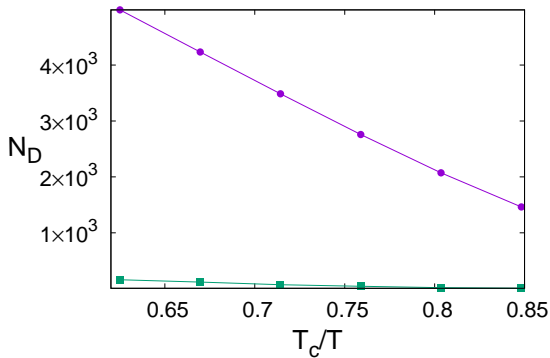


FIG. 9. N_D from Monte Carlo simulations for $2D$ -XY model. The lower curve corresponds to estimate from KM.

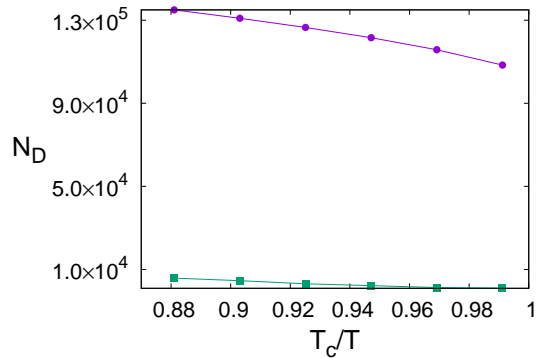


FIG. 10. N_D from Monte Carlo simulations for $3D$ -XY model. The lower curve corresponds to estimate from KM.

C. Distribution of vortices in two spatial dimensions

In this section the results on the distribution of vortices are presented for two spatial dimensions. Each of the configuration in the thermal ensemble, generated using the Monte Carlo simulations, is analysed to compute the number of defects and net winding number inside a 100×100 sub-lattice, which is quarter of the full system. Within this sub-lattice each elementary squares is scanned for vortices. To determine if there is a defect inside a square the Geodesic rule is applied to specify field variations between NN points. This uniquely determines the winding number of the field along the perimeter. The variations of θ along a closed path on the lattice is a topological number, i.e $2\pi n$ for integer n . If the θ of the spins varies by $(-)2\pi$ as the perimeter is traced once in the clockwise direction, the winding is considered to be $(-)1$. The net winding on the full lattice is zero as the the lattice is effectively a torus (T^2) due to periodic boundary conditions imposed along the x, y directions. Fig.9 shows, N_D , the average number of vortices and anti-vortices in the whole lattice. For comparison we compute defects inside each elementary square in three dimensional lattice ignoring the sign of the winding number. The results are shown in Fig.10. In both cases the number of vortices decreases with temperature. In Fig.9 and Fig.10, the estimates using the KM are also included, which underestimate N_D by large margins for temperatures considered here.

The number of vortices for all temperatures $T > T_c$, is way above what is expected from the Kibble Mechanism. It can be easily shown that the probability of having a vortex

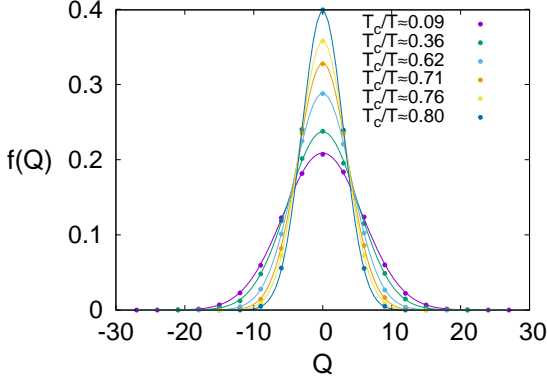


FIG. 11. The distributions of the net winding number in the sub-lattice at various temperatures.

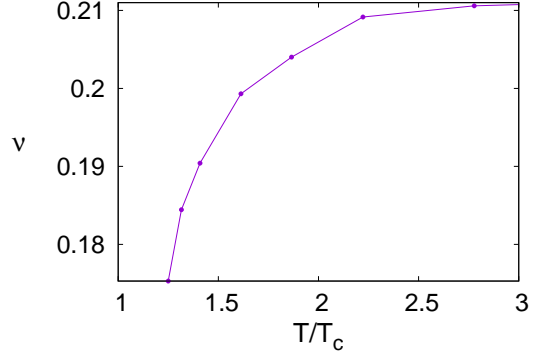


FIG. 12. The exponent ν corresponding to the standard deviation in the net winding number distributions.

or anti-vortex inside an equilateral triangle of size ξ_{KM} is $1/4$ [19]. If the Geodesic rule is violated by 50% then this probability that there is a defect inside the triangle goes up to $5/8$. This suggests that at finite temperature most of the defects are created via thermal fluctuations. For example, at $T = 1.18$, using the Geodesic rule or it's violation by 50%, the maximum number of defects expected inside the sub-lattice is about ~ 27 when ξ_{KM} is used for the estimate. The average number of defects in this case is ~ 700 . This discrepancy reduces when standard correlation length, ξ , and the probability that the Geodesic rule is violated at this temperature are considered.

D. Correlation between vortices and anti-vortices

The Kibble Mechanism predicts strong correlation among the vortices [6]. It is expected that, given a vortex the probability that the nearest defect is an anti-vortex is higher than a vortex. This can be deduced from the Kibble Mechanism in the following way [6, 28]. The number of defects within an area A is $N \sim A/\xi^2$. On the other hand the perimeter of this area is $\sim A^{1/2}$. This can be traversed in $N^{1/2} \sim A^{1/2}/\xi$ steps of length ξ . Since for each step the average variation of θ is $\pi/2$, the net variation of θ along the perimeter can be computed using method of random walk of $N^{1/2}$ steps. Hence it is expected that the standard deviation is $\sim N^\nu$ with $\nu = 1/4$. For a completely random distribution of vortices $\nu = 1/2$. In Fig.11 we plot the distribution of net winding number in the sub-lattice for various temperatures.

The distributions shown in Fig.11 can be fitted well with gaussians. The exponent ν is given by the standard deviation of the gaussians. The resulting values of ν extracted for various temperatures is shown in Fig.12. The exponent ν for $T = 1.18$ turns out to be 0.18. For $T = 2.5$, $\nu \simeq 0.21$. Note that a constant factor is to be taken into account while comparing these results with the the Kibble Mechanism [6]. The resulting ν approaches the value $1/4$ for $T \rightarrow \infty$. This makes sense as the geodesic rule is imposed at the scale of lattice spacing and the NN spins are uncorrelated in this limit. In the following we study the Geodesic rule in ϕ^4 theory. The results are qualitatively similar to the present case of $O(2)$ -spins.

III. GEODESIC RULE IN ϕ^4 THEORY

The lattice action for the ϕ^4 theory with $U(1)$ symmetry is taken to be,

$$S_\phi = -\kappa \sum_{i,\mu} \left(\phi_i^\dagger \phi_{i+\hat{\mu}} + h.c \right) + \sum_i \left[\frac{1}{2} \phi_i^\dagger \phi_i + \lambda \left(\phi_i^\dagger \phi_i - 1 \right)^2 \right] \quad (6)$$

where $\mu = x, y, z$. $\hat{\mu}$ represent the unit vector in the μ -th direction. λ represents the coupling for the quartic self-interaction of the ϕ field. λ is fixed to 1 for the simulations. The NN coupling parameter κ plays the role of inverse temperature in this case. The corresponding partition function is given by

$$\mathcal{Z} = \int \prod_i d\phi_i^* d\phi_i \text{Exp}[-S_\phi]. \quad (7)$$

The field ϕ being complex can be thought of as a two component vector, whose magnitude can fluctuate unlike in the case of $O(2)$ -spins. In the thermodynamic limit the system undergoes a $2nd$ order phase transition at κ_c . The paramagnetic phase persists upto κ_c . For $\kappa > \kappa_c$ the system is found to be in the ferromagnetic phase.

The equilibrium configurations in this model are generated by using the pseudo heat-bath algorithm. In this algorithm to update ϕ_i an action S_i is considered, which is obtained from S_ϕ by dropping term which does not depend on ϕ_i . The resulting action S_i is rewritten as a sum of gaussian in ϕ_i and a quartic term. The gaussian term is used to generate a new ϕ_i which is accepted with probability determined by the change in the quartic term.

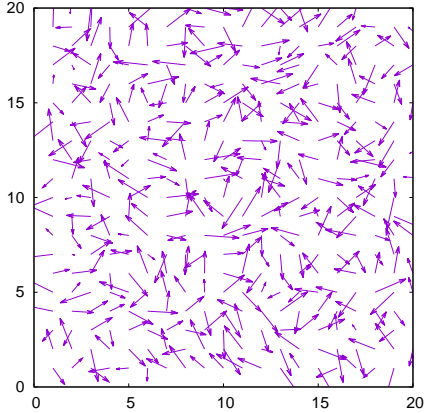


FIG. 13. A sampled spin configuration at $T = 2T_c$.

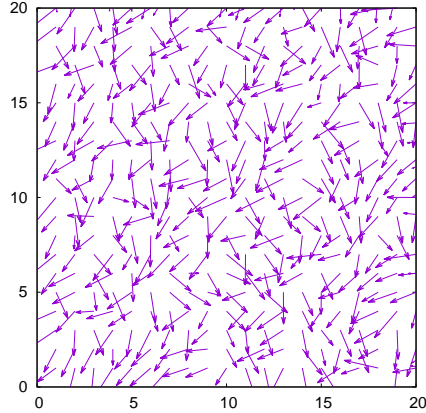


FIG. 14. A sampled spin configuration at $T = 0.76T_c$.

This process is repeated to update ϕ at all the lattice sites. To reduce the auto correlation over relaxation method is used. In addition every 5th configuration is used for analysis. For details see reference [29]. The simulations are carried out for $60 \times 60 \times 60$ 3D lattice. The Fig.13 and Fig.14 show two dimensional section of typical field configurations at $\kappa = 0.15$ and $\kappa = 0.4$ respectively.

At high temperatures, $\kappa < \kappa_c$, the volume and thermal average of ϕ is zero, however $\phi_i = 0$ is suppressed due to vanishing measure. It is found that the image trajectory, of any field configuration over a linear stretch r , rarely passes through the origin ($\phi = 0$) in the field space. Therefore the phase θ of the field ϕ can be used for the computation of the probability of deviation from the Geodesic rule following the procedures adopted in the case of $O(2)$ -spins. $\Delta\theta_{ij}$ and η_{ij} are found as function of the separation $r = |\mathbf{r}_i - \mathbf{r}_j|$. As in the case of $O(2)$ spins whenever $\Delta\theta_{ij} \neq \eta_{ij}$ the Geodesic rule is considered to be violated. The Fig.15 shows the probability of deviation from the Geodesic rule as function of r for different κ . The deviation increases with r and temperature $1/\kappa$ similar to the case of $O(2)$ -spins. The red squares on the curves correspond to the deviation at $r = \xi_{KM}$.

IV. CONCLUSIONS

We have studied the variations of field in the XY -model in two and three dimensions and ϕ^4 theory in three dimensions using Monte Carlo lattice simulations. For two dimensions the lattice size was taken to be 200×200 . For three dimensions we consider 60^3 lattice.

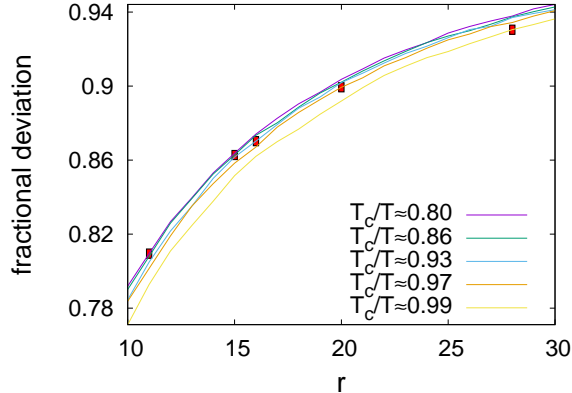


FIG. 15. Geodesic rule deviation for ϕ^4 theory.

The computations are carried out above the critical temperature to check the validity of the Geodesic rule used in the Kibble-Zurek mechanism of defect formation in 2nd order phase transitions. For this purpose a correlation length ξ_{KM} is defined using the criteria that field correlation vanish approximately. This length scale is different from the conventional correlation length ξ . At ξ separations the field can not be considered uncorrelated which is crucial for the Geodesic rule. It is found that even at ξ separations the field variation deviates significantly from what is expected from the Geodesic rule. At ξ_{KM} separations non geodesic paths are found to be equally or more probable than the geodesic paths.

We also studied the number of vortices and the net winding number in the case of $O(2)$ -spins in two dimensions. The geodesic rule is assumed for field variations between nearest neighbour spins. This is necessary to probe the location and winding charge of the vortices. The analysis is carried out a sub-lattice of size 100×100 which is a quarter of the whole lattice. This is necessary as in this case the net winding number is not constrained to be zero. The number of vortices is found to be significantly higher than what is expected from the Kibble-Zurek mechanism. The discrepancy does not improve much even after the deviation from the geodesic rule is incorporated in the Kibble-Zurek mechanism. The simulation results show that the large number of vortices are a result of the thermal production. This is supported by results of the distribution of the net winding number. The results show that the corresponding standard deviation is much smaller than what is expected from the consideration of the Geodesic rule. This result suggests that there is significant pairing between the vortices and anti-vortices. It is expected that from topological considerations thermal fluctuations always form pair of vortex-anti-vortex and at smaller separations. We

mention here that in theories with gauge symmetries there is no satisfactory argument for the Geodesic rule [30]. The trajectory of the field between two domains can be deformed by gauge transformations. The Monte Carlo simulation method presented here can be extended to settle the Geodesic rule in these theories, which we plan to do next.

ACKNOWLEDGMENTS

We thank A. P. Balachandran, Ajit. M. Srivastava and Rajarshi Ray for valuable comments.

REFERENCES

- [1] I. Chuang, B. Yurke, R. Durrer and N. Turok, *Science* **251**, 1336-1342 (1991)
doi:10.1126/science.251.4999.1336
- [2] P.C. Hendry et al, *Nature (London)* 368, 315 (1994) doi:10.1038/368315a0
- [3] V.M.H. Ruutu et al, *Nature(London)* 382, 334 (1996) doi:10.1038/382334a0
- [4] C. Bäuerle et al., *Nature* 382 (1996) 332 doi:10.1038/382332a0
- [5] M. E. Dodd, P. C. Hendry, N. S. Lawson, P. V. E. McClintock and C. D. H. Williams, *Phys. Rev. Lett.* **81**, no.17, 3703-3706 (1998) doi:10.1103/PhysRevLett.81.3703 [arXiv:cond-mat/9808117 [cond-mat.soft]].
- [6] S. Dital, R. Ray and A. M. Srivastava, *Phys. Rev. Lett.* **83**, 5030 (1999) doi:10.1103/PhysRevLett.83.5030 [arXiv:hep-ph/9805502 [hep-ph]].
- [7] R. Carmi, E. Polturak and G. Koren, *Phys. Rev. Lett.* **84**, 4966-4969 (2000) doi:10.1103/PhysRevLett.84.4966
- [8] M. B. Hindmarsh and T. W. B. Kibble, *Rept. Prog. Phys.* **58**, 477-562 (1995) doi:10.1088/0034-4885/58/5/001 [arXiv:hep-ph/9411342 [hep-ph]].
- [9] J. Magueijo and R. H. Brandenberger, [arXiv:astro-ph/0002030 [astro-ph]].
- [10] A. M. Srivastava, P. Bagchi, A. Das and B. Layek, *Pramana* **89**, no.4, 68 (2017) doi:10.1007/s12043-017-1465-1

- [11] S. Digal, R. Ray, S. Sengupta and A. M. Srivastava, Phys. Rev. Lett. **84**, 826-829 (2000) doi:10.1103/PhysRevLett.84.826 [arXiv:hep-ph/9911446 [hep-ph]].
- [12] W. H. Zurek, W. H. Zurek, Nature (London) **317**, 505 (1985) doi:10.1038/317505a0; Phys. Rept. **276**, 177-221 (1996) doi:10.1016/S0370-1573(96)00009-9 [arXiv:cond-mat/9607135 [cond-mat]].
- [13] G. Toulouse, M. Kléman. Journal de Physique Lettres, Edp sciences, 1976, 37 (6), pp.149-151. doi:10.1051/jphyslet:01976003706014900. jpa-00231261
- [14] N. D. Mermin, Rev. Mod. Phys. **51**, 591-648 (1979) doi:10.1103/RevModPhys.51.591
- [15] Srivastava A.M. (2001) Topological Defects in Condensed Matter Physics. In: Field Theories in Condensed Matter Physics. Texts and Readings in Physical Sciences doi:10.1007/978-93-86279-07-1 5
- [16] Paul M Chaikin, T C Lubensky; Principles of condensed matter physics, Cambridge, Cambridge University Press, 1995, ISBN:0 521 43224 3
- [17] T. W. B. Kibble, J. Phys. A **9**, 1387-1398 (1976) doi:10.1088/0305-4470/9/8/029
- [18] T. W. B. Kibble and A. Vilenkin, Phys. Rev. D **52**, 679-688 (1995) doi:10.1103/PhysRevD.52.679 [arXiv:hep-ph/9501266 [hep-ph]].
- [19] M. J. Bowick, L. Chandar, E. A. Schiff and A. M. Srivastava, Science **263**, 943-945 (1994) doi:10.1126/science.263.5149.943 [arXiv:hep-ph/9208233 [hep-ph]].
- [20] R. Ray and A. M. Srivastava, Phys. Rev. D **69**, 103525 (2004) doi:10.1103/PhysRevD.69.103525 [arXiv:hep-ph/0110165 [hep-ph]].
- [21] A. M. Srivastava, Phys. Rev. D **46**, 1353-1367 (1992) doi:10.1103/PhysRevD.46.1353
- [22] S. Chakravarty and A. M. Srivastava, Nucl. Phys. B **406**, 795-807 (1993) doi:10.1016/0550-3213(93)90010-M [arXiv:hep-ph/9209246 [hep-ph]].
- [23] E. J. Copeland and P. M. Saffin, Phys. Rev. D **54**, 6088-6094 (1996) doi:10.1103/PhysRevD.54.6088 [arXiv:hep-ph/9604231 [hep-ph]].
- [24] S. Digal, S. Sengupta and A. M. Srivastava, Phys. Rev. D **56**, 2035-2043 (1997) doi:10.1103/PhysRevD.56.2035 [arXiv:hep-ph/9705246 [hep-ph]].
- [25] S. Digal and A. M. Srivastava, Phys. Rev. Lett. **76**, 583-586 (1996) doi:10.1103/PhysRevLett.76.583 [arXiv:hep-ph/9509263 [hep-ph]].
- [26] J. M. Kosterlitz and D. J. Thouless, J. Phys. C **6**, 1181-1203 (1973) doi:10.1088/0022-3719/6/7/010

- [27] Hasting W.K., “Monte Carlo sampling methods using Markov chains and their applications”;
Biometrika 57 (1970) 97–109, doi:10.1093/biomet/57.1.97
- [28] T. Vachaspati and A. Vilenkin, Phys. Rev. D **30**, 2036 (1984) doi:10.1103/PhysRevD.30.2036
- [29] B. Bunk, Nucl. Phys. B Proc. Suppl. **42**, 566-568 (1995) doi:10.1016/0920-5632(95)00313-X
- [30] S. Rudaz and A. Mohan Srivastava, Mod. Phys. Lett. A **8**, 1443-1450 (1993)
doi:10.1142/S0217732393001161 [arXiv:hep-ph/9212279 [hep-ph]].